

Antiangiogenic therapy with Nintedanib affects hypoxia, angiogenesis and apoptosis in the ventral prostate of TRAMP animals

Raquel Frenedoso da Silva, Thais Petrochelli Banzato, Letícia Ferreira Alves, João Ernesto Carvalho, Rajesh Agarwal, et al.

Cell and Tissue Research

ISSN 0302-766X

Cell Tissue Res

DOI 10.1007/s00441-019-03091-x



Your article is protected by copyright and all rights are held exclusively by Springer-Verlag GmbH Germany, part of Springer Nature. This e-offprint is for personal use only and shall not be self-archived in electronic repositories. If you wish to self-archive your article, please use the accepted manuscript version for posting on your own website. You may further deposit the accepted manuscript version in any repository, provided it is only made publicly available 12 months after official publication or later and provided acknowledgement is given to the original source of publication and a link is inserted to the published article on Springer's website. The link must be accompanied by the following text: "The final publication is available at link.springer.com".



Antiangiogenic therapy with Nintedanib affects hypoxia, angiogenesis and apoptosis in the ventral prostate of TRAMP animals

Raquel Frenedoso da Silva^{1,2} · Thais Petrochelli Banzato³ · Leticia Ferreira Alves¹ · João Ernesto Carvalho^{3,4} · Rajesh Agarwal² · Valéria Helena Alves Cagnon¹

Received: 13 November 2018 / Accepted: 7 August 2019
© Springer-Verlag GmbH Germany, part of Springer Nature 2019

Abstract

The antiangiogenic therapy for prostate cancer with Nintedanib, a potent inhibitor of important growth factor receptors, has been proven to delay tumor progression and arrest tumor growth; thus, the aim herein is to evaluate Nintedanib effects on tumor cells, besides angiogenesis and apoptosis processes, metalloproteinases and hypoxia factor in an animal model. Nintedanib promoted growth inhibition and cell death in a dose-dependent manner, showing no tumor selectivity. Transgenic Adenocarcinoma of the Mouse Prostate (TRAMP) were treated with Nintedanib (10 mg/kg/day) in different stages of tumor development and the ventral prostate was examined for protein levels by means of immunohistochemistry and Western blotting and apoptosis evaluation. In vitro antiproliferative activity of Nintedanib was also assessed in nine human tumor cell lines. Early Nintedanib treatment has shown decreased levels of FGF-2, VEGFR-1, MMP-9 and HIF-1 α and a significantly increased apoptosis of epithelial cells. Furthermore, late Nintedanib treatment decreased FGF-2, VEGFR-1 and FGFR-3 levels. Importantly, even after treatment discontinuation, treated animals displayed a significant decrease in VEGFR-1 as well as MMP-9. Although Nintedanib treatment in late stages of tumor growth has shown some good results, it is noteworthy that the drug presents the best tissue response when administered in the early stages of disease development. Nintedanib treatment has shown to be a promising approach for prostate cancer therapy, especially in the early stages of the disease, interfering in different carcinogenesis progression pathways.

Keywords Angiogenesis · Prostate cancer · Growth factors · Tumor cells · Nintedanib

Electronic supplementary material The online version of this article (<https://doi.org/10.1007/s00441-019-03091-x>) contains supplementary material, which is available to authorized users.

✉ Valéria Helena Alves Cagnon
quitete@unicamp.br

Raquel Frenedoso da Silva
raquelfrenedoso@yahoo.com.br

Thais Petrochelli Banzato
thaisbanzato@gmail.com

Leticia Ferreira Alves
leferralves@gmail.com

João Ernesto Carvalho
carvalho@cpqba.unicamp.br

Rajesh Agarwal
rajesh.agarwal@ucdenver.edu

¹ Department of Structural and Functional Biology, Institute of Biology, State University of Campinas (UNICAMP), P.O. Box 6109, Campinas, São Paulo 13083-865, Brazil

² Department of Pharmaceutical Sciences, Skaggs School of Pharmacy, University of Colorado Anschutz Medical Campus, Aurora, CO, USA

³ Chemical, Biological and Agricultural Pluridisciplinary Research Center, State University of Campinas (UNICAMP), São Paulo, Brazil

⁴ Faculty of Pharmaceutical Sciences, State University of Campinas (UNICAMP), São Paulo, Brazil

Introduction

Prostate cancer is the second most common malignancy diagnosed in men, especially over the age of 65 years. In 2018, more than 164,000 new cases of the disease were estimated only in the United States, resulting in more than 29,000 deaths (Siegel et al. 2018). The disease develops after destabilization of the pro- and anti-apoptotic balance, which may be due to genetic or environmental changes, leading to the uncontrolled growth of epithelial cells and proceeding towards carcinoma (Hanahan and Weinberg 2011). The carcinoma progression might be enhanced by androgen influence, given the importance of such hormone in the prostate physiology (Goncalves et al. 2013).

It is well known that changes in lifestyle, such as physical activity and consumption of fruits and vegetables, may be helpful for prostate cancer prevention. Otherwise, if the disease is already in the advanced stages, radical prostatectomy might be necessary. However, the surgery is accompanied with severe side effects, such as urinary incontinence and impotence, impairing patients' quality of life (Daniyal et al. 2014). The most usual treatment for prostate cancer is hormone therapy, named androgen deprivation therapy, which reduces the levels of male hormones affecting prostate cells (Yamaguchi et al. 2014). However, androgen deprivation effects might disappear after therapy discontinuation and the disease often progresses to castration-resistant prostate cancer (CRPC), showing poor prognosis (Xu et al. 2017).

Angiogenesis, the process of new blood formation around a tumor, has a central role in CRPC; thus, great effort has been made to quest for new antiangiogenic drugs, which have been proven to be an effective treatment strategy for prostate cancer in different stages of development (Mukherji et al. 2013). The discovery of drugs that target and inhibit the action of angiogenic factors, such as vascular endothelial growth factor (VEGF) and fibroblast growth factor (FGF), is an important focus of studies, since these factors are implicated in tumor progression and metastasis (Doll et al. 2001). Nintedanib, a new intracellular angiokinase inhibitor, has shown an ability to target multiple tyrosine kinase receptors, inhibiting the pro-angiogenic pathways mediated by not only VEGF but also FGF and platelet-derived growth factor (PDGF) receptors, preventing tumor growth by suppressing angiogenesis (McCormack 2015).

The importance of a triple inhibitor, such as Nintedanib, is that, during tumor progression, the angiogenesis process may be regulated by multiple pathways that can compensate for each other when only one of them is the target of chemotherapy (Awasthi and Schwarz 2015). Kudo et al. (2011) showed that Nintedanib *in vivo* in the doses of 50 to 100 mg/kg/day reduced tumor growth in nude mice inoculated with hepatocarcinoma cells (Kudo et al. 2011). Furthermore, Nintedanib treatment reduced tumor volume in nude mice

inoculated with head and neck and kidney carcinoma cells (Hilberg et al. 2008).

Recent studies from our research group, using the Transgenic Adenocarcinoma of the Mouse Prostate (TRAMP) model, have shown that treatment with 10 mg/kg/day of Nintedanib orally delayed prostate cancer progression by decreasing pro-angiogenic protein levels and interfering with androgen receptor in the prostatic ventral lobe after the same treatment regimen was used in the present study (da Silva et al. 2017). Furthermore, Nintedanib has proven its anti-inflammatory action on the anterior prostate, decreasing COX-2 and IL-17 levels and altering extracellular matrix components (da Silva et al. 2017; Alves et al. 2018; Nogueira Pangrazi et al. 2018). Importantly, Nintedanib reduced cell proliferation even when the treatment is discontinued, showing to be non-toxic for the liver (da Silva et al. 2017).

Considering that Nintedanib inhibits a wide variety of receptors and the treatment regimen for patients is not well established yet, it is important to assess whether the drug is more effective on blocking angiogenesis during the early or late stages of tumor development. Thus, the aim herein was to evaluate the Nintedanib effects on angiogenesis-related molecules as well as apoptosis, metalloproteinases and hypoxia factor in the ventral prostate of TRAMP animals that received treatment during different stages of tumor development for four weeks. Furthermore, the antiproliferative activity of Nintedanib was evaluated on nine human tumor cell lines and one non-tumor cell line.

Material and methods

In vitro studies

Antiproliferative activity of Nintedanib in human cancer cells

Nintedanib antiproliferative activity was assessed *in vitro*, using Doxorubicin (Europharma, 0.025, 0.25, 2.5 and 25 $\mu\text{g}/\text{mL}$) as positive control, in nine different human cancer cell lines—lung non-small cell (NCI-H460), ovarian-expressing multiple drug-resistant phenotype (NCI-ADR/RES), ovarian (OVCAR-3), colon (HT29), glioblastoma (U251), melanoma (UACC-62), prostate (PC-3), leukemia (K-562) and kidney (786-0) (100 μL suspension/well)—at 37 °C and 5% CO₂, 35% humidity. After 24 h of incubation, the cells were treated, in triplicate, for 48 h with Nintedanib diluted in DMSO (concentration did not affect cell viability (0.1%, Merck®) in three different concentrations (0.25, 2.5 and 25 $\mu\text{g}/\text{mL}$).

In order to evaluate the cellular response for total growth inhibition (TGI, value representing the needed concentration ($\mu\text{g}/\text{mL}$) to completely inhibit cancer cell proliferation), cell population density was recorded at time zero (time when the

drug was added; T₀ plate), in order to compare with the population density at the end of the experiment. Then, the cells were fixed with 50% trichloroacetic acid and cell proliferation was spectrophotometrically determined (540 nm) by using sulforhodamine B (SRB) (Monks et al. 1991). The TGI (calculated from T = T₀, being T the amount of protein at the end of treatment), LC₅₀ (drug concentration promoting 50% of cell death) and GI₅₀ (concentration inhibiting 50% of cell growth) were determined through non-linear regression analysis using the concentration–response curve for each cell line in software ORIGIN 8.0® (OriginLab Corporation). The experiment was carried out in triplicate. All the cell lines used in this study were provided by the National Cancer Institute, Frederick (MA, USA) and maintained in CPQBA—Chemical, Biological and Agricultural Pluridisciplinary Research Center at the University of Campinas (UNICAMP), Brazil.

In vivo studies

The TRAMP animals (C57BL/6-Tg (TRAMP) 8,247Ng/JX FVB/JUnib) were from the Multidisciplinary Center for Biological Investigation in Laboratory Animal Science at the State University of Campinas (UNICAMP) and received water and solid food ad libitum (Nuvilab, Colombo, PR, Brazil). The Ethics Committee on Animal Use (CEUA-UNICAMP) approved this study under the protocol number 3285-1, carried out in agreement with the Ethical Principles for Animal Research established by the Brazilian College for Animal Experimentation (COBEA).

The treated animals received Nintedanib (ApexBio®) orally at 10 mg/kg/day diluted in vehicle (Tween 20, 10%) and the control animals received vehicle only, for four weeks. The experimental groups were defined as follows ($n = 11$): control and Nintedanib groups receiving early treatment, from 8 to 12 weeks of age and euthanized at the end of the treatment (TC12 and TN12, respectively) or at 22 weeks of age (TC22(8–12) and TN22(8–12), respectively) and control and Nintedanib groups receiving late treatment, from 12 to 16 weeks of age and euthanized at the end of the treatment (TC16 and TN16, respectively) or at 22 weeks of age (TC22(12–16) and TN22(12–16), respectively). Furthermore, TRAMP animals were euthanized at 8 weeks of age (T8) in order to establish the initial lesion grade, when the treatments mentioned previously had started (Fig. S1).

At the end of the treatment periods, the animals were weighed in *Denver P-214* scale (Denver Instrument Company, Arvada, CO, USA) and anesthetized with 2% xylazine hydrochloride (5 mg/kg; Konig, São Paulo, Brazil) and 10% ketamine hydrochloride (60 mg/kg; Fort Dodge, IA) for further euthanasia. Samples of ventral prostate were collected and submitted to immunohistochemistry and protein

level analyses by means of Western blotting and apoptosis assay.

Apoptosis detection

Three samples of the ventral prostate lobe of each experimental group were collected and fixed in paraformaldehyde 4% for 12 h. Afterwards, the samples were dehydrated in increasing concentration of ethanol, diaphanized in xylene and embedded in plastic resin (Paraplast Plus, St. Louis). Five-micrometer-thick sections were obtained using a microtome (Zeiss Hyrax M60) and the sections were deparaffinized in xylene, hydrated in a decreasing ethanol series, rinsed under distilled water and submitted to DNA fragmentation detection using Dead-end Fluorometric TUNEL system (Promega, Madison, WI, USA) following the manufacturer's protocol. The apoptotic nuclei were identified and photographed through inverted microscope Olympus IX71-II (Olympus, CA, USA) equipped with fluorescence (IX2-FL-II, Olympus, CA, USA). For nuclear staining, the slides were incubated with DAPI at 0.5 µg/mL for 15 min. The images taken (10 fields per animal, totalizing 30 fields per experimental group) were analyzed using a multipoint system with 400 intersections (modified from Weibel 1963). The number of apoptotic cells was determined by counting of positive nucleus staining coinciding with grade intersection divided by the total number of points coinciding with DAPI-stained nucleus. The results were expressed in relative frequency of positive staining in all the experimental groups.

Immunohistochemistry

The samples of the ventral prostate lobe of five animals per group were collected, fixed in Bouin and submitted to immunohistochemistry. Antigens were retrieved by boiling the sections in 10 mM citrate buffer (pH 6.0) followed by endogenous peroxidase blocking in H₂O₂. After that, the sections were incubated in a blocking solution (BSA in TBS-T buffer) for 1 h at room temperature in order to block non-specific binding. Then, the antigens FGF-2, FGF-7, VEGFR-1, FGFR-3, MMP-9 and HIF-1α were localized through immunostaining with the following antibodies: rabbit polyclonal (sc-79) (Santa Cruz Biotechnology, USA), goat polyclonal (sc-1365) (Santa Cruz Biotechnology, USA), rabbit polyclonal (sc-316) (Santa Cruz Biotechnology, USA), rabbit polyclonal antibody (sc-123) (Santa Cruz Biotechnology, USA), goat polyclonal (sc-6840) (Santa Cruz Biotechnology, USA) and mouse monoclonal (sc-53546) (Santa Cruz Biotechnology, USA), respectively, diluted in BSA 1% and incubated overnight at 4 °C. Negative controls were

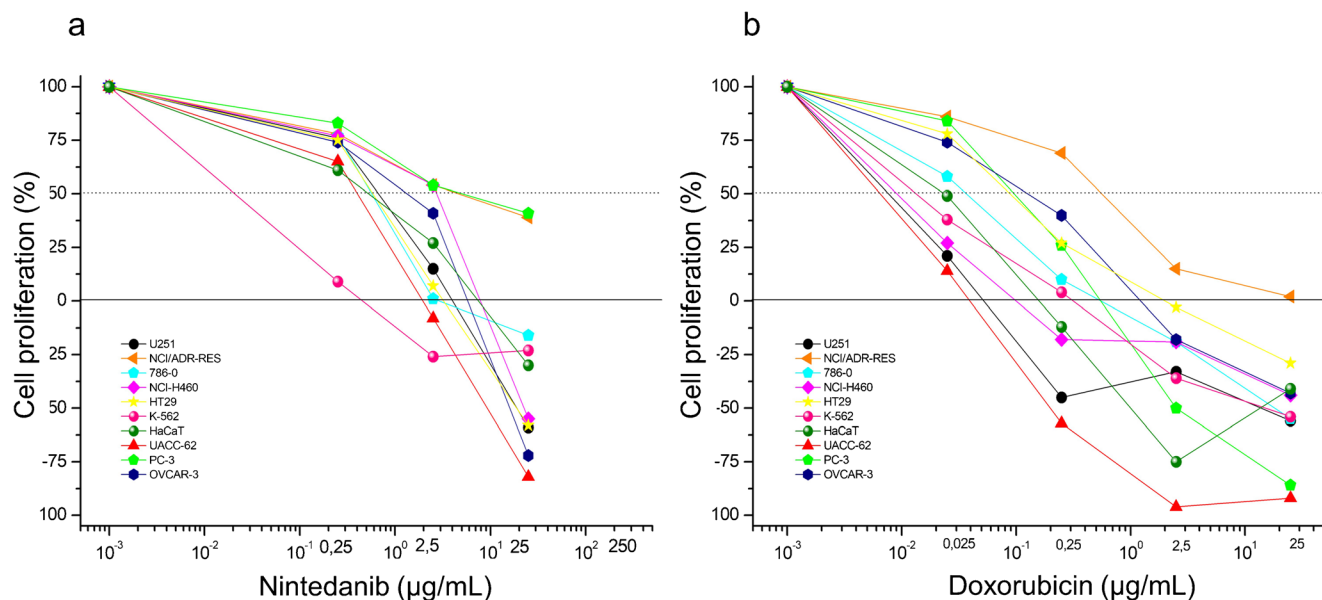


Fig. 1 Antiproliferative activity of Nintedanib (a) and positive control Doxorubicin (b) in nine human tumor cell lines and one non-tumor (HaCat). The dashed lines represent GI50 while continuous lines represent TGI

incubated only with PBS under identical conditions (Supplementary Fig. 1b). After TBS-T washing, the slides were incubated with the proper HRP-conjugated secondary antibody and peroxidase activity was detected using diaminobenzidine (DAB) chromogenic (Sigma-Aldrich, St. Louis, MO). The samples were counter-stained with Harris hematoxylin and the photographs (10 fields per animal, totalizing 50 fields per experimental group) were taken under 400× magnification in a photomicroscope Nikon Eclipse E-400 (Nikon, Japan). The prostatic tissue was evaluated using a multipoint system with 400 intersections (modified from Weibel 1963). The results were determined by immunoreactivity count coinciding with the grid intersection divided by the total number of points

Table 1 Average GI50, TGI and LC50 of nine human tumor cell lines and one non-tumor (HaCat) after Nintedanib exposure from 0.25 to 25 µg/mL

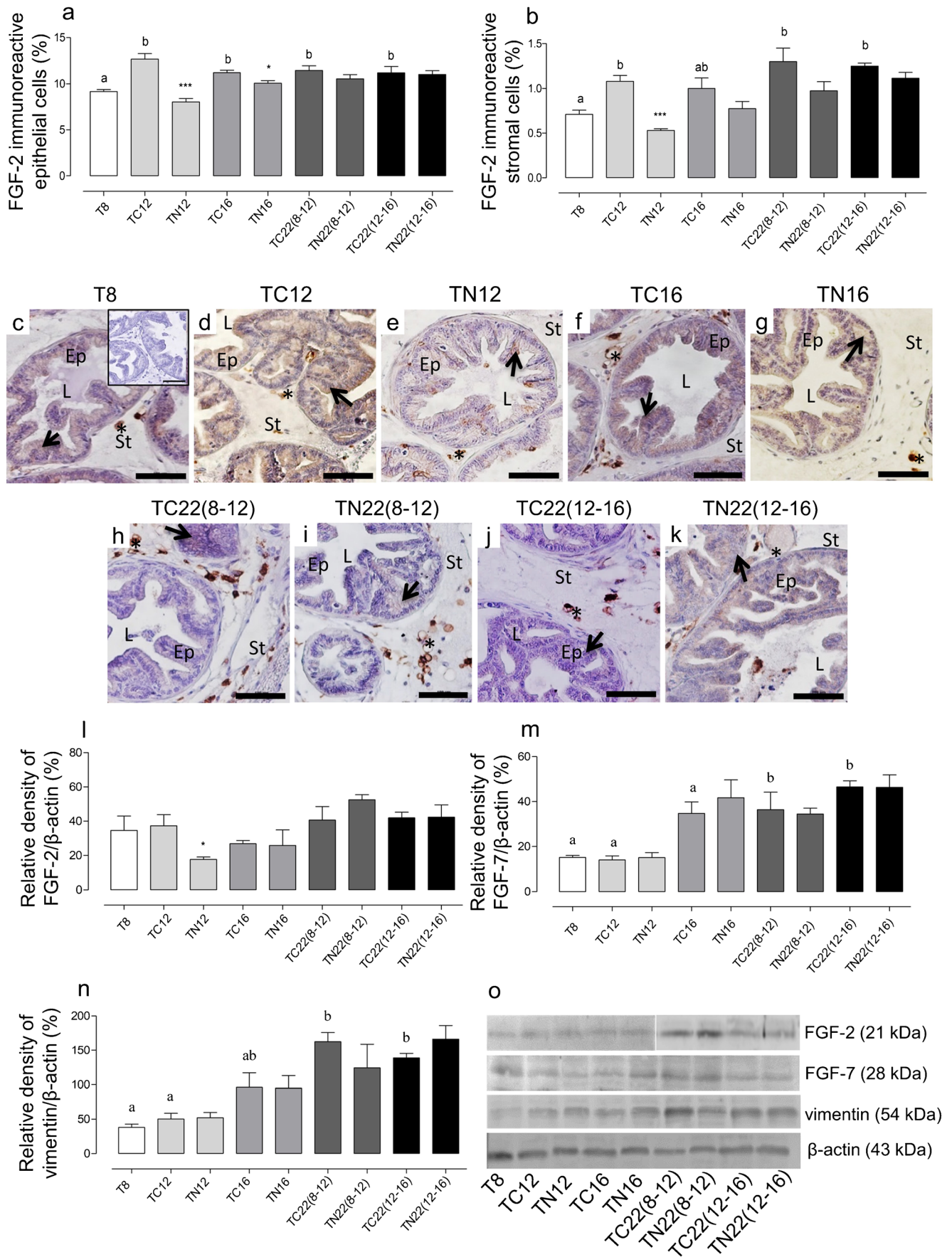
Cell line	GI50 (µg/mL)	TGI (µg/mL)	LC50 (µg/mL)
U251	0.57	3.82	23.84
UACC	0.27	1.90	2.74
NCI/ADR-RES	5.81	> 250	> 250
786-0	0.40	6.99	34.92
NCI-H460	2.55	7.50	24.42
PC-3	7.08	> 250	> 250
OVCA3	2.46	5.08	22.20
HT29	2.29	3.35	5.79
K-562	0.18	0.38	> 250
HaCaT	0.46	7.05	28.18

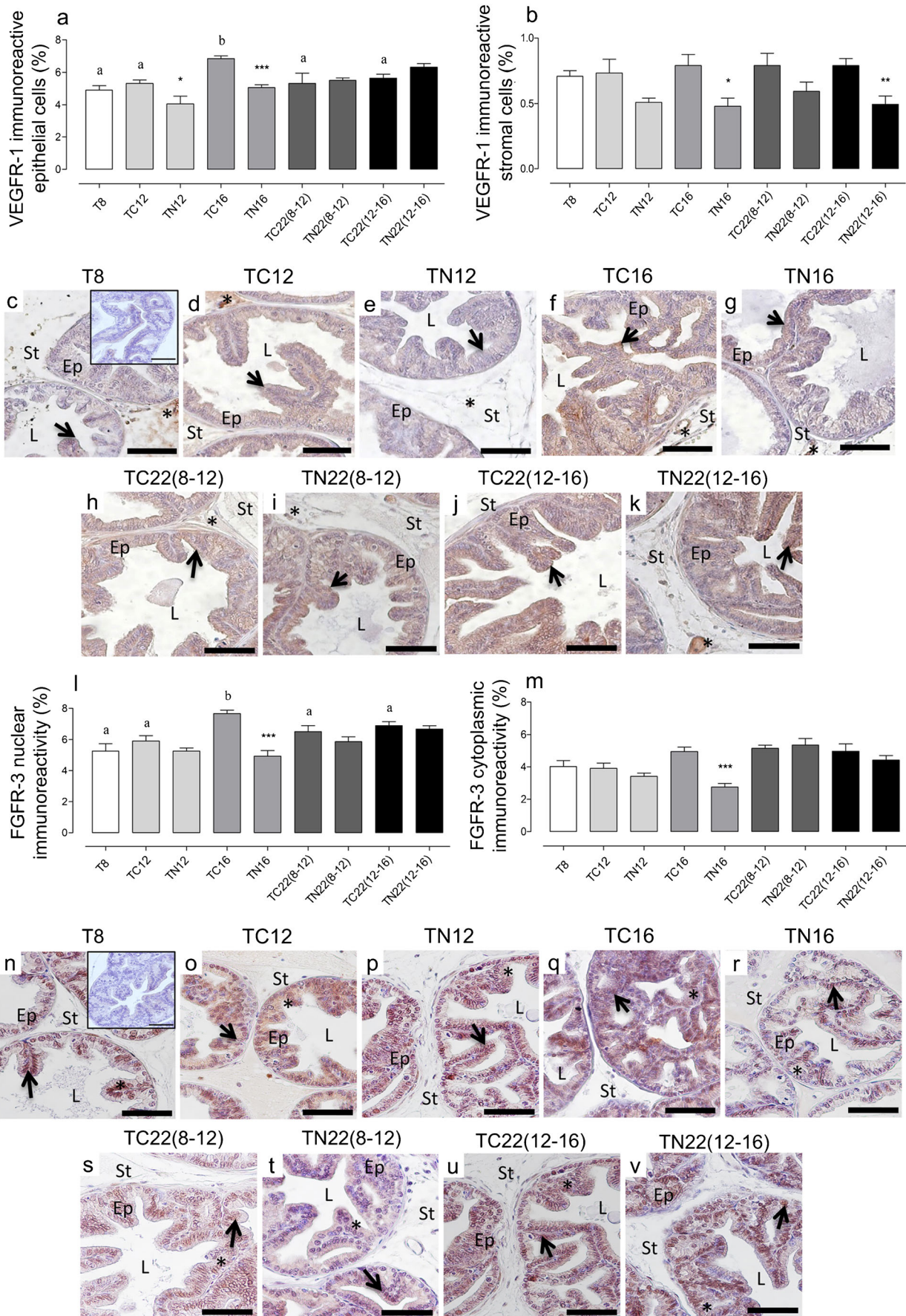
and expressed as a relative frequency of positive staining for each molecule in all the experimental groups.

Western blotting

The samples of the ventral prostate lobe from three animals per group were collected and homogenized in a Polytron homogenizer (Kinematica Inc., Lucerne, Switzerland) in a 40 mL/mg protein extraction buffer for 1 min. The tissue extracts were obtained by centrifuging the samples for 20 min (14,000 rpm at 4 °C) and used for protein quantification with Bradford’s reagent (Bio-Rad Laboratories, Hercules, CA). After that, the supernatant was mixed (1:1) with 3× Laemmli buffer and transferred to a dry bath at 100 °C for 5 min; 75 µg of protein was submitted to separation according to molecular weight in SDS-PAGE gels under reducing conditions. Proteins were transferred to Hybond-ECL nitrocellulose membranes (Amersham, Pharmacia Biotech, Arlington Heights, IL) at 120 V for 90 min. The membranes were blocked with BSA diluted in TBS-T for 1 h and incubated with FGF-2

Fig. 2 FGF-2 immunostaining in epithelial (a) and stromal cells (b), respectively. FGF-2 photomicrographs of different experimental groups (c–k). Values expressed as media ± S.E.M. of five. Positive immunostaining is indicated by an arrow in the epithelium and asterisk in the stroma. Ep, epithelium; St, stroma; L, lumen. Counter-staining: Harris hematoxylin. Scale bar: 100 µm. Protein levels of FGF-2 (l), FGF-7 (m) and vimentin (n) in the ventral prostate of TRAMP animals (values related to β-actin and expressed as media ± S.E.M. of the three). Representative bands of FGF-2, FGF-7, vimentin and β-actin (o). Asterisks indicate significant difference between treated group and its respective control group and different letters indicate significant difference among control groups. **p* < 0.05; ***p* < 0.01; ****p* < 0.005





◀ **Fig. 3** VEGFR-1 immunostaining in epithelial (a) and stromal cells (b), respectively. VEGFR-1 photomicrographs of different experimental groups (c–k). Positive immunostaining is indicated by an arrow in the epithelium and asterisk in the stroma. FGFR-3 immunostaining in nucleus (l) and cytoplasm (m) of epithelial cells, respectively. FGFR-3 photomicrographs of different experimental groups (n–v). Positive immunostaining is indicated by an arrow in the nucleus and asterisk in the cytoplasm. Values expressed as media ± S.E.M. of five. Ep, epithelium; St, stroma; L, lumen. Counter-staining: Harris hematoxylin. Scale bar: 100 μm. Asterisks indicate significant difference between treated group and its respective control group and different letters indicate significant difference among control groups. * $p < 0.05$; ** $p < 0.01$; *** $p < 0.005$

and FGF-7 (described previously) and mouse monoclonal (ab8069) for Vimentin. After washing with TBS-T, the membranes were incubated with the proper secondary antibody and the peroxidase activity was developed with the chemiluminescent solution (Pierce Biotechnology, Rockford, IL) for 5 min, followed by fluorescence capture using the Gene Gnome equipment and the GeneSys image acquisition software (Syngene Bio Imaging, Cambridge, UK). An endogenous control for comparison among groups was used (mouse monoclonal anti-β-actin (sc-81178); Santa Cruz Biotechnology, CA and the results were determined by densitometry using ImageJ (image analysis and processing in Java) software for image analyses and expressed in relation to endogenous control band intensity.

Statistical analyses

ANOVA followed by the test of Bonferroni was used to compare data among control groups and two-tailed *t* test was used to compare data between the treated group and its respective control group. Differences were considered significant when $p < 0.05$ and data are presented as mean ± standard error of the mean (S.E.M.) (Zar 1999). The statistical analyses were performed by the software GraphPad Prism (version 5.0).

Results

Nintedanib exposure decreased cell proliferation and induced cell death in different human tumor cells

The antiproliferative effects of the drug on human tumor cells are shown in (Fig. 1a). The lowest Nintedanib dose (0.25 μg/mL) decreased cell proliferation in all human tumor cell lines, showing its cytostatic effect. Exposure to 2.5 μg/mL of Nintedanib continued to inhibit cell proliferation in seven tumor cell lines (PC3, NCI-ADR/RES, NCI-H460, OVCAR-3, HT29, U251, 786-0) but, importantly, it led to cell death in the two remaining (K-562 and

UACC-62). Furthermore, 25 μg/mL of Nintedanib treatment displayed cell death in seven cell lines (except PC3 and NCI-ADR/RES), showing the drug's cytotoxic effect on different tumor cells (Fig. 1a). The antiproliferative effects of positive control Doxorubicin are shown in (Fig. 1b). Considering the GI50 average activity, four tumor cell lines (K-562, UACC-62, 786-0 and U251) exhibited GI50 values between 0.18 and 0.57 μg/mL, while, for the other cell lines, the values were between 2.29 and 7.08 μg/mL (Table 1).

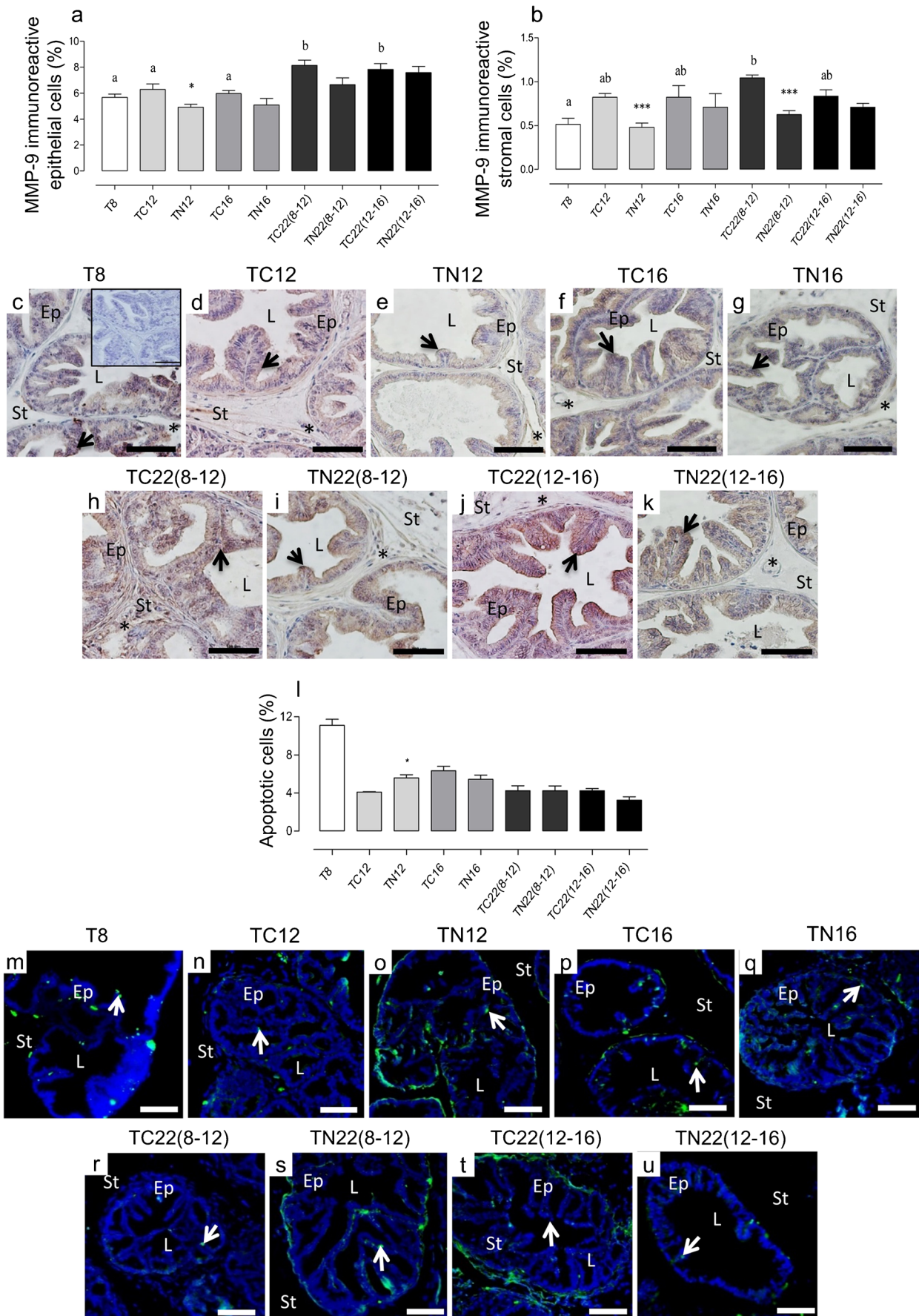
Nintedanib treatment in the early stages of cancer development in the TRAMP mice was able to significantly decrease the levels of angiogenesis-related and matrix degradation proteins as well as increase apoptosis

The TN12 group animals showed a significant decrease in FGF-2 in both prostatic compartments (Fig. 2a–e), besides a significant decrease in epithelial VEGFR-1 compared to the TC12 group (Fig. 3a,d,e). There was no effect in FGFR-3 immunolocalization in the early treatment groups TC12 and TN12 (Fig. 3l,m). There was a significant MMP-9 decrease after Nintedanib treatment in the TN12 group in both epithelial and stromal cells (Fig. 4a,b,d,e). Interestingly, the T8 group animals displayed an expressive number of apoptotic cells, an effect no longer observed after 12 weeks of age (Fig. 4l,m). There was a significant increase in apoptosis after early treatment with Nintedanib, as observed in the TN12 group (Fig. 4l,n,o). There was no difference in FGF-7 (Fig. 2m, Fig. 5a,b) and vimentin (Fig. 2n) levels in the prostate of the TN12 group compared to those of TC12. A significant reduction in the HIF-1α levels in the prostatic epithelium of animals receiving early Nintedanib treatment (TN2 group) was observed (Fig. 5l,n,o).

Late treatment with Nintedanib decreased pro-angiogenic molecules in the ventral prostate of TRAMP animals

A significant decrease in the epithelial FGF-2 levels was observed after late Nintedanib treatment (Fig. 2a,f,g). A peak of VEGFR-1 levels was observed in 16 weeks of age (TC16) animals in the epithelium, which was significantly reduced after Nintedanib treatment in the TN16 group as well as a significant reduction in the stromal cells in the same group (Fig. 3a,b,f,g).

FGFR-3 nuclear levels were significantly increased in 16 weeks of age animal (TC16) and, after late Nintedanib treatment, a significant reduction in FGFR-3 levels was observed in both the nucleus and cytoplasm (Fig. 3l,m,q,r). There were no differences between the TC16 and TN16



◀ **Fig. 4** MMP-9 immunostaining in epithelial (a) and stromal cells (b), respectively. MMP-9 photomicrographs of different experimental groups (c–k). Values expressed as media ± S.E.M. of five. Positive immunostaining is indicated by an arrow in the epithelium and asterisk in the stroma; counter-staining: Harris hematoxylin. Epithelial apoptotic cells in different experimental groups (l) and its photomicrographs (m–u). Values expressed as media ± S.E.M. of three. Ep, epithelium; St, stroma; L, lumen. Scale bar: 100 μm. Asterisks indicate a significant difference between the treated group and its respective control group and different letters indicate significant difference among control groups. * $p < 0.05$; ** $p < 0.01$; *** $p < 0.005$

groups regarding MMP-9, HIF-1 α and apoptosis levels (Fig. 4a,b,l and Fig. 5l). FGF-7 and vimentin levels were significantly increased after 16 weeks of age in the TRAMP animals; however, no effects were observed after Nintedanib treatment (Fig. 2m,n and Fig. 5a,b,f,g).

Animals from both groups receiving early and late treatments and maintained without receiving a drug up to 22 weeks of age, showed important alterations regarding angiogenesis and matrix remodeling

Despite Nintedanib treatment interruption for 6 weeks prior to euthanasia, the animals from the group TN22(12–16) displayed a significant decrease in VEGFR-1 levels in the stromal cells when compared to the control group (Fig. 3b,j,k). Importantly, the decreased MMP-9 stromal levels observed in the early treatment group were maintained even after treatment suspension for 10 weeks in the TN22(8–12) group when compared to the TC22(8–12) group (Fig. 4b,h,i).

Discussion

Herein, we have assessed which tumor cell lines could respond to treatment through analysis of antiproliferative activity *in vitro*, since recent studies have shown that Nintedanib decreased proliferation of tumor cells dependent on the angiogenic pathway (Awasthi et al. 2015; Steinemann et al. 2016). We have previously shown reduced tumor cell proliferation *in vivo* after Nintedanib treatment (da Silva et al. 2017). Accordingly, our results showed that the drug exerted its cytostatic effect on reducing cell proliferation in all human tumor cells, without selectivity for a specific cell line, including the non-tumor HaCat. Furthermore, increasing doses of Nintedanib was able to cause cell death in several tumor cell lines; however, this effect was less pronounced in PC3 cells, which, curiously, showed the same pattern of inhibition observed for multiple drug-resistant phenotype cell lines (NCI-ADR/RES). Corroborating our present findings, a recent study showed that for human prostate cancer cells, increased concentrations of Nintedanib are needed to induce cell death

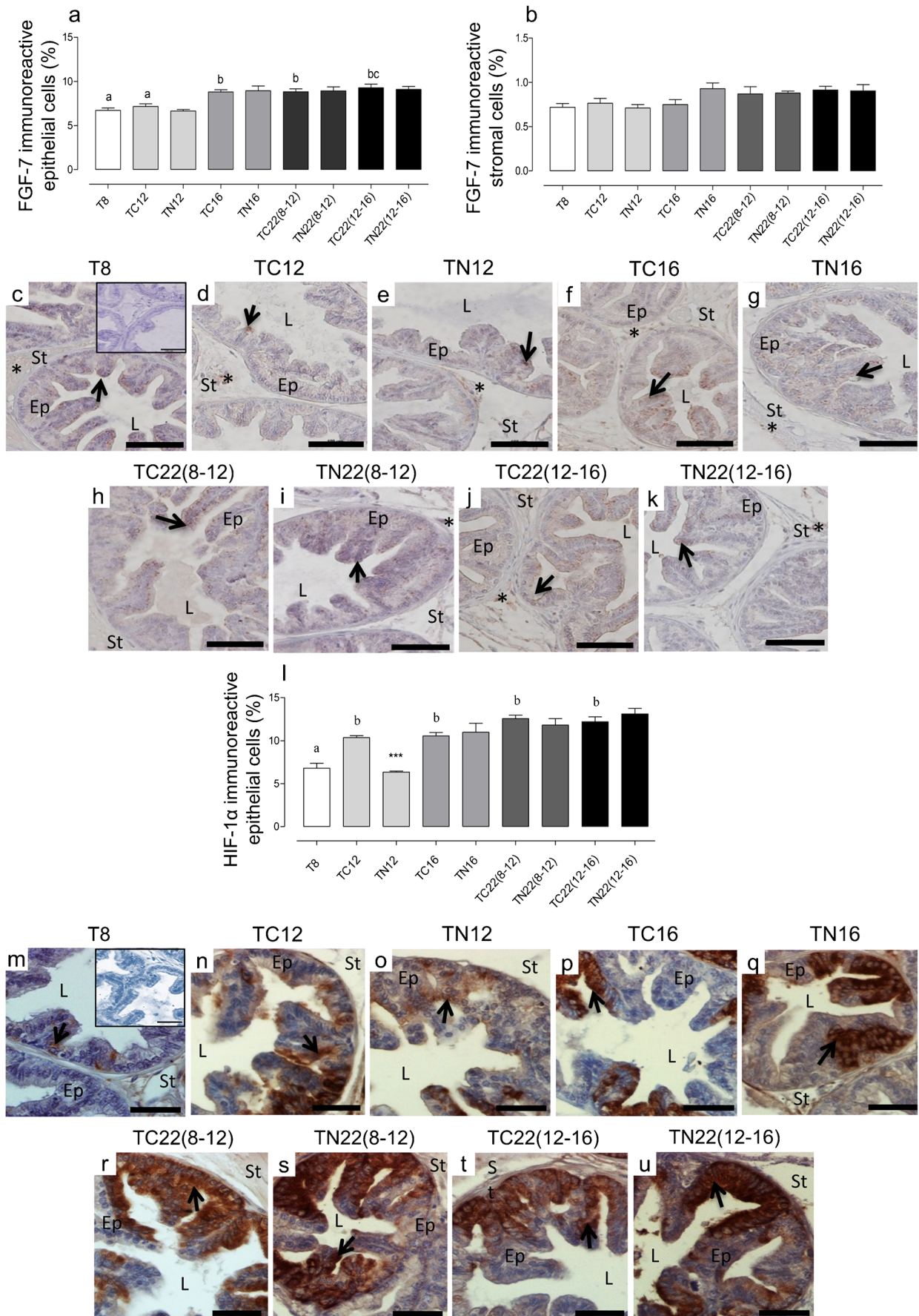
in both androgen-dependent and -independent cell lines; otherwise, at 2.5 and 5 μM, Nintedanib only inhibited cell proliferation (da Silva et al. 2018).

Our findings herein showed that both growth factors and their receptors are increased during prostate tumor progression in TRAMP mice, promoting the stimulation of the angiogenesis process, as well as extracellular matrix remodeling and hypoxia condition. Also, we showed that in early tumor development, there was an elevated level of apoptotic epithelial cells. Nintedanib treatment pointed out promising results when the drug administration happened in the early stages of disease development, since it decreased the growth factor levels and their receptors in the ventral prostate of the treated animals as well as decreasing MMP-9 and HIF-1 α levels and increasing apoptotic cell number. Interestingly, some of these effects remained even after treatment interruption.

During tumor development, FGF-2 expression is increased in the prostate of both humans (Giri et al. 1999) and TRAMP mice (Huss et al. 2003), showing its involvement in carcinogenesis. Indeed, the present results showed that there were increased levels of this molecule in the TRAMP mouse ventral prostate, in both epithelium and stroma glandular. Thus, based on our results, we can indicate that the increased FGF-2 secretion in the stroma during cancer might act as a growth factor for epithelial cells, contributing to its disordered growth and proliferation. Polnaszek et al. (2003) showed that the knockout of FGF-2 in TRAMP mice delays tumor progression (Polnaszek et al. 2003). Our findings, showing reduced FGF-2 levels in the prostate stroma and epithelium of animals receiving early Nintedanib treatment, support this idea, as does our previous findings on delayed tumor progression at the same treatment regimen (da Silva et al. 2017).

Hernandez and colleagues showed for the first time the molecular changes in FGFR-3 in human prostatic disorders (Lo Iacono et al. 2016). The authors demonstrated a prevalence of FGFR-3 mutations in low-grade tumors, indicating the central role of this receptor in prostate neoplasia initiation (Hernandez et al. 2009; Lo Iacono et al. 2016); we found increased FGFR-3 levels with aging in the TRAMP mouse prostate, reaching a significantly high peak of expression at 16 weeks of age. A subsequent decrease with increasing age was observed, when cancer progresses to a more advanced stage, corroborating some studies that showed that FGFR-3 is not overexpressed neither in benign prostatic hyperplasia nor in prostate cancer itself (Boget et al. 2001; Gowardhan et al. 2005; Sahadevan et al. 2007).

Importantly, Nintedanib treatment significantly decreased FGFR-3 levels in TRAMP animals at 16 weeks of age, in both nucleus and cytoplasm, which collaborates with decreased angiogenesis in the tissue. Our results are in agreement with Feng et al. (2012), which showed marked inhibition of



◀ **Fig. 5** FGF-7 immunostaining in epithelial (a) and stromal cells (b), respectively. FGF-7 photomicrographs of different experimental groups (c–k). Positive immunostaining is indicated by an arrow in the epithelium and asterisk in the stroma. HIF-1 α immunostaining in epithelial cells (l). HIF-1 α photomicrographs of different experimental groups (m–u). Positive immunostaining is indicated by an arrow in the nucleus and asterisk in the cytoplasm. Positive immunostaining is indicated by an arrow. Values expressed as media \pm S.E.M. of five. Ep, epithelium; St, stroma; L, lumen. Counter-staining: Harris hematoxylin. Scale bar: 100 μ m. Asterisks indicate significant difference between the treated group and its respective control group and different letters indicate a significant difference among control groups. * p < 0.05; ** p < 0.01; *** p < 0.005

angiogenesis and proliferation and increasing cell death rates, after inhibition of FGFR-1 and FGFR-4, both in vitro (PNT1a cells) and in vivo (VCaP xenograft model) (Feng et al. 2012). These results led the authors to believe that blocking FGFR signaling significantly reduces tumor growth and could be an interesting approach for prostate cancer treatment (Feng et al. 2012; Feng et al. 2017).

Overexpression of VEGFR-1, present in both vascular-endothelial cells and epithelial tumor cells, has been considered a hallmark of the disease, being correlated with increased cell proliferation and metastatic potential, besides poor prognosis (Ferrara et al. 2003; Ruggeri et al. 2003). As a matter of fact, we noticed in the present results an increased epithelial VEGFR-1 expression as time progresses and the disease develops in TRAMP animals up to 16 weeks of age, suggesting the activation of this receptor might be crucial to signaling pathways leading to cancer progression; after this period, VEGFR-1 levels declined.

Even though Nintedanib had some effectiveness on decreasing VEGFR-1 after early treatment, the main influence of the drug was observed after late treatment regimen, for there was a significant decrease in VEGFR-1 levels in both epithelium and stroma and, importantly, the stromal decrease persisted even after treatment interruption. Decreased VEGFR-1-positive cells might be crucial at the late stages of prostate cancer development, since studies have pointed out that they hold a niche for premetastatic tumor cells. Therefore, their suppression would improve the clinical outcome (Pal et al. 2015).

Huss et al. (2001) showed that, in TRAMP mouse, increased HIF-1 α expression is an early event during cancer development, since the angiogenic switch is driven by this factor. Our previous study showed that increased VEGF levels in the prostate ventral lobe are associated with advanced stages of tumor development (da Silva et al. 2017). In the same manner, results presented herein showed that tumor progression in the TRAMP mouse prostate could be stimulated by increased levels of both FGF-2 and HIF-1 α with advanced age. Taken together, these findings demonstrate that targeting the angiogenesis signaling induced by hypoxia may be an effective strategy towards prostate cancer treatment.

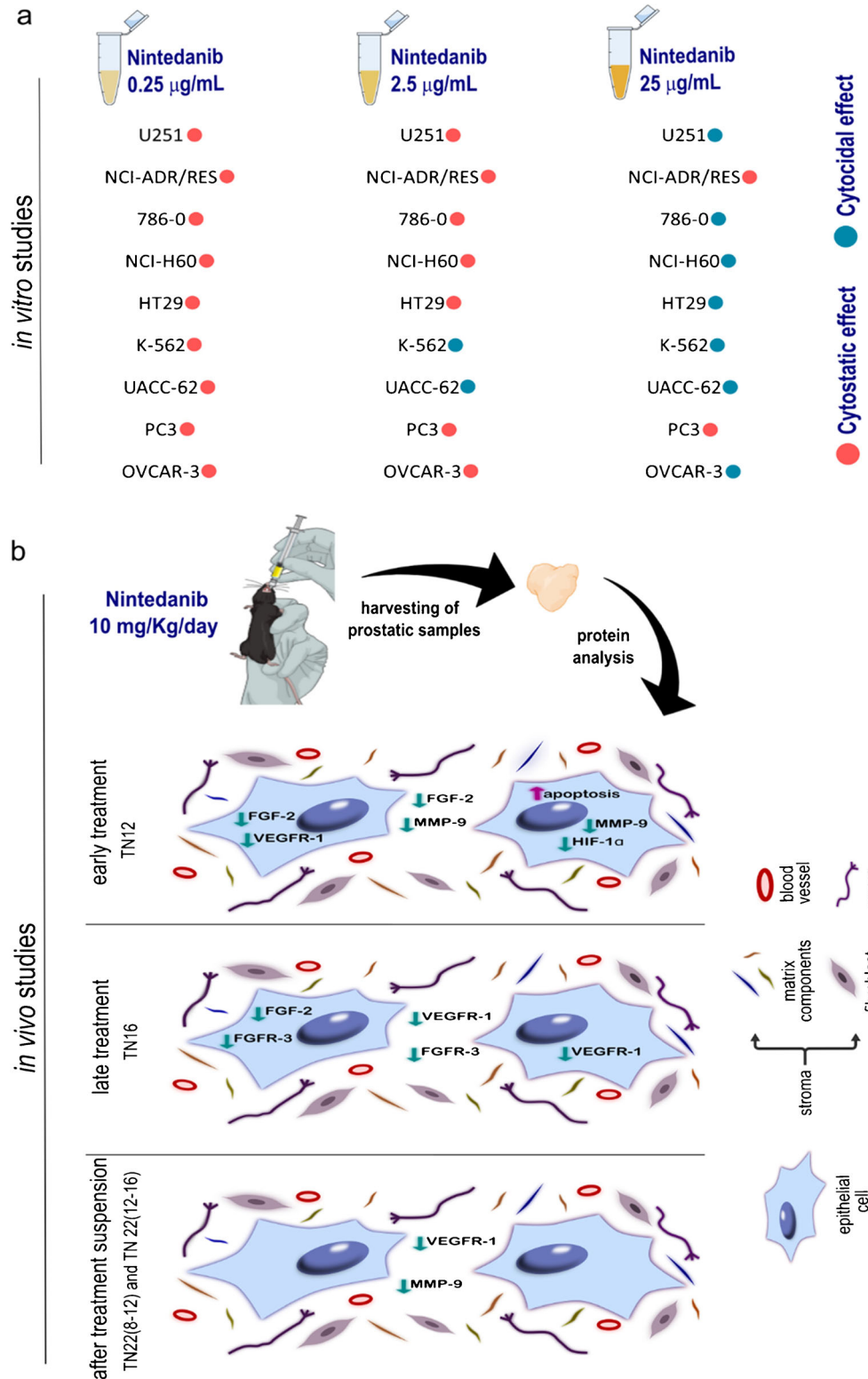
Thus, it is noteworthy that, in the present study, Nintedanib treatment in the early stages of tumor development significantly decreased HIF-1 α levels in the prostate epithelium, which might explain the reduced levels of FGF-2 and VEGF herewith and previously observed after the same treatment (da Silva et al. 2017).

Alterations in structural proteins are not limited to epithelial cells during tumor development, as they also befall in the stromal cells during stroma remodeling, such as increased MMP expression. This increase is often associated with prostate cancer progression, since they are responsible for extracellular matrix degradation during tumorigenesis, contributing to increased tumor cell invasiveness (Castellano et al. 2008; Damasceno et al. 2014; Noh et al. 2015). Accordingly, we observed increased MMP-9 levels in the prostate of TRAMP mouse as the animals progressively present a more aggressive phenotype of the disease. Corroborating our present results, a study from our research group showed that the MMP-9 expression was significantly increased at 18-week-old TRAMP mice in both the epithelium and prostatic stroma (Montico et al. 2014). In the present study, Nintedanib treatment interfered with stroma remodeling, since it significantly reduced MMP-9 levels, especially in the early treatment regimen with the drug. More importantly, these effects remained even when the treatment was discontinued for 10 weeks prior to the euthanasia.

Initially, the increased apoptosis rates during cancer occur as an attempt to protect the tissues by eliminating potentially malignant cells (Labi and Erlacher 2015). Accordingly, we observed in the present study an elevated apoptosis rate at the beginning of neoplasia development in the 8 weeks of age TRAMP animals, suggesting the compensative action of this process in trying to eliminate mutated epithelial cells. Conversely, a differential role for increased apoptosis during tumor development, in a process termed death-driven proliferation, in which dying cells stimulate cell division and proliferation of surrounding cells in the tumor by secreting mitogen factors, has been discussed (Mollereau et al. 2013), pointing out the role of apoptosis in unrestrained proliferation observed in the TRAMP mouse prostate. However, the apoptosis rate decreased as time progresses up to 22 weeks of age in these animals, as observed in the present study, showing that malignant cells acquire resistance and might evade apoptosis during tumor progression, for this response prevents cancer cells from effective elimination by anticancer mechanisms (Lowe and Lin 2000).

In summary, we provided evidence that Nintedanib exposure caused both cytotoxic and cytostatic effects in different tumor cell lines (Fig. 6a). Treatment of animals with the drug decreased angiogenesis-related growth factors and their receptors, such as FGF-2, FGFR-3 and VEGFR-1, in the ventral prostate of TRAMP mouse, possibly by inhibiting

Fig. 6 Summary scheme of in vitro and in vivo data after Nintedanib exposure, showing cytostatic and cytotoxic effects of the drug in different tumor cells (a) and the changes in the epithelium and stroma of prostate microenvironment (b). The stromal components (fibroblasts, matrix components, blood vessels and autonomic nerves) and the epithelial cells (blue) are not to scale. Figure created using components of the “Mind the Graph” and “Inkscape” platforms



the hypoxia condition, as shown by decreased HIF-1 α expression, which ultimately interfered with stroma remodeling and increased apoptosis of prostate tumor cells (Fig. 6b).

Altogether, these changes might lead to delay in prostate cancer development and progression. Thus, Nintedanib treatment has shown to be a promising approach for prostate cancer

therapy, especially in the early stages of the disease, interfering in different carcinogenesis progression pathways.

Acknowledgments Not applicable.

Authors' contribution Study design, collection, analyses and interpretation of data and writing of manuscript: Raquel Frenedoso da Silva and Valéria Helena Alves Cagnon. Collection and analyses of data: Thais Petrochelli Banzato and Letícia Ferreira Alves. Analyses and interpretation of data: Rajesh Agarwal and João Ernesto Carvalho.

Funding This work was supported by a grant from the São Paulo Research Foundation (FAPESP 2013/26677-7) and in part by the NCI R01 grant CA195708 (to RA).

Compliance with ethical standards

Conflict of interest The authors declare that there is no conflict of interest that could be perceived as prejudicing the impartiality of the research reported.

Ethical approval The Ethics Committee on Animal Use (CEUA-UNICAMP) approved this study under protocol number 3285-1, carried out in agreement with the Ethical Principles for Animal Research established by the Brazilian College for Animal Experimentation (COBEA).

References

- Alves LF, da Silva RF, Cagnon VHA (2018) Nintedanib effects on delaying cancer progression and decreasing COX-2 and IL-17 in the prostate anterior lobe in TRAMP mice. *Tissue Cell* 50:96–103
- Awasthi N, Schwarz RE (2015) Profile of nintedanib in the treatment of solid tumors: the evidence to date. *Onco Targets Ther* 8:3691–3701
- Awasthi N, Hinz S, Brekken RA, Schwarz MA, Schwarz RE (2015) Nintedanib, a triple angiokinase inhibitor, enhances cytotoxic therapy response in pancreatic cancer. *Cancer Lett* 358:59–66
- Boget S, Cereser C, Parvaz P, Leriche A, Revol A (2001) Fibroblast growth factor receptor 1 (FGFR1) is over-expressed in benign prostatic hyperplasia whereas FGFR2-IIIc and FGFR3 are not. *Eur J Endocrinol* 145:303–310
- Castellano G, Malaponte G, Mazzarino MC, Figini M, Marchese F, Gangemi P, Travali S, Stivala F, Canevari S, Libra M (2008) Activation of the osteopontin/matrix metalloproteinase-9 pathway correlates with prostate cancer progression. *Clin Cancer Res* 14:7470–7480
- da Silva RF, Nogueira-Pangrazi E, Kido LA, Montico F, Arana S, Kumar D, Raina K, Agarwal R, Cagnon VHA (2017) Nintedanib antiangiogenic inhibitor effectiveness in delaying adenocarcinoma progression in Transgenic Adenocarcinoma of the Mouse Prostate (TRAMP). *J Biomed Sci* 24:31
- da Silva RF, Dhar D, Raina K, Kumar D, Kant R, Cagnon VHA, Agarwal C, Agarwal R (2018) Nintedanib inhibits growth of human prostate carcinoma cells by modulating both cell cycle and angiogenesis regulators. *Sci Rep* 8:9540
- Damasco AA, Carvalho CP, Santos EM, Botelho FV, Araujo FA, Deconte SR, Tomiosso TC, Balbi AP, Zanon RG, Taboga SR, Goes RM, Ribeiro DL (2014) Effects of maternal diabetes on male offspring: high cell proliferation and increased activity of MMP-2 in the ventral prostate. *Cell Tissue Res* 358:257–269
- Daniyal M, Siddiqui ZA, Akram M, Asif HM, Sultana S, Khan A (2014) Epidemiology, etiology, diagnosis and treatment of prostate cancer. *Asian Pac J Cancer Prev* 15:9575–9578
- Doll JA, Reiher FK, Crawford SE, Pins MR, Campbell SC, Bouck NP (2001) Thrombospondin-1, vascular endothelial growth factor and fibroblast growth factor-2 are key functional regulators of angiogenesis in the prostate. *Prostate* 49:293–305
- Feng S, Shao L, Yu W, Gavine P, Ittmann M (2012) Targeting fibroblast growth factor receptor signaling inhibits prostate cancer progression. *Clin Cancer Res* 18:3880–3888
- Feng S, Shao L, Castro P, Coleman I, Nelson PS, Smith PD, Davies BR, Ittmann M (2017) Combination treatment of prostate cancer with FGF receptor and AKT kinase inhibitors. *Oncotarget* 8:6179–6192
- Ferrara N, Gerber HP, LeCouter J (2003) The biology of VEGF and its receptors. *Nat Med* 9:669–676
- Giri D, Ropiquet F, Ittmann M (1999) Alterations in expression of basic fibroblast growth factor (FGF) 2 and its receptor FGFR-1 in human prostate cancer. *Clin Cancer Res* 5:1063–1071
- Goncalves BF, de Campos SG, Zanetoni C, Scarano WR, Falleiros LR Jr, Amorim RL, Goes RM, Taboga SR (2013) A new proposed rodent model of chemically induced prostate carcinogenesis: distinct time-course prostate cancer progression in the dorsolateral and ventral lobes. *Prostate* 73:1202–1213
- Gowardhan B, Douglas DA, Mathers ME, McKie AB, McCracken SR, Robson CN, Leung HY (2005) Evaluation of the fibroblast growth factor system as a potential target for therapy in human prostate cancer. *Br J Cancer* 92:320–327
- Hanahan D, Weinberg RA (2011) Hallmarks of cancer: the next generation. *Cell* 144:646–674
- Hernandez S, de Muga S, Agell L, Juanpere N, Esgueva R, Lorente JA, Mojal S, Serrano S, Lloreta J (2009) FGFR3 mutations in prostate cancer: association with low-grade tumors. *Mod Pathol* 22:848–856
- Hilberg F, Roth GJ, Krssak M, Kautschitsch S, Sommergruber W, Tontsch-Grunt U, Garin-Chesa P, Bader G, Zoephel A, Quant J, Heckel A, Rettig WJ (2008) BIBF 1120: triple angiokinase inhibitor with sustained receptor blockade and good antitumor efficacy. *Cancer Res* 68:4774–4782
- Huss WJ, Hanrahan CF, Barrios RJ, Simons JW, Greenberg NM (2001) Angiogenesis and prostate cancer: identification of a molecular progression switch. *Cancer Res* 61:2736–2743
- Huss WJ, Barrios RJ, Foster BA, Greenberg NM (2003) Differential expression of specific FGF ligand and receptor isoforms during angiogenesis associated with prostate cancer progression. *Prostate* 54:8–16
- Kudo K, Arai T, Tanaka K, Nagai T, Furuta K, Sakai K, Kaneda H, Matsumoto K, Tamura D, Aomatsu K, De Velasco MA, Fujita Y, Saijo N, Kudo M, Nishio K (2011) Antitumor activity of BIBF 1120, a triple angiokinase inhibitor and use of VEGFR2+Tyr+ peripheral blood leukocytes as a pharmacodynamic biomarker in vivo. *Clin Cancer Res* 17:1373–1381
- Labi V, Erlacher M (2015) How cell death shapes cancer. *Cell Death Dis* 6:e1675
- Lo Iacono M, Buttigliero C, Monica V, Bollito E, Garrou D, Cappia S, Rapa I, Vignani F, Bertaglia V, Fiori C, Papotti M, Volante M, Scagliotti GV, Porpiglia F, Tucci M (2016) Retrospective study testing next generation sequencing of selected cancer-associated genes in resected prostate cancer. *Oncotarget* 7:14394–14404
- Lowe SW, Lin AW (2000) Apoptosis in cancer. *Carcinogenesis* 21:485–495
- McCormack PL (2015) Nintedanib: first global approval. *Drugs* 75:129–139
- Mollereau B, Perez-Garijo A, Bergmann A, Miura M, Gerlitz O, Ryoo HD, Steller H, Morata G (2013) Compensatory proliferation and apoptosis-induced proliferation: a need for clarification. *Cell Death Differ* 20:181

- Monks A, Scudiero D, Skehan P, Shoemaker R, Paull K, Vistica D, Hose C, Langley J, Cronise P, Vaigro-Wolff A et al (1991) Feasibility of a high-flux anticancer drug screen using a diverse panel of cultured human tumor cell lines. *J Natl Cancer Inst* 83:757–766
- Montico F, Kido LA, Hetzl AC, Lorencini RM, Candido EM, Cagnon VH (2014) Antiangiogenic therapy effects on age-associated matrix metalloproteinase-9 (MMP-9) and insulin-like growth factor receptor-1 (IGFR-1) responses: a comparative study of prostate disorders in aged and TRAMP mice. *Histochem Cell Biol* 142:269–284
- Mukherji D, Temraz S, Wehbe D, Shamseddine A (2013) Angiogenesis and anti-angiogenic therapy in prostate cancer. *Crit Rev Oncol Hematol* 87:122–131
- Nogueira Pangrazi E, da Silva RF, Kido LA, Montico F, Cagnon VHA (2018) Nintedanib treatment delays prostate dorsolateral lobe cancer progression in the TRAMP model: contribution to the epithelial-stromal interaction balance. *Cell Biol Int* 42:153–168
- Noh EM, Park YJ, Kim JM, Kim MS, Kim HR, Song HK, Hong OY, So HS, Yang SH, Kim JS, Park SH, Youn HJ, You YO, Choi KB, Kwon KB, Lee YR (2015) Fisetin regulates TPA-induced breast cell invasion by suppressing matrix metalloproteinase-9 activation via the PKC/ROS/MAPK pathways. *Eur J Pharmacol* 764:79–86
- Pal SK, Vuong W, Zhang W, Deng J, Liu X, Carmichael C, Ruel N, Pinnamaneni M, Twardowski P, Lau C, Yu H, Figlin RA, Agarwal N, Jones JO (2015) Clinical and translational assessment of VEGFR1 as a mediator of the premetastatic niche in high-risk localized prostate cancer. *Mol Cancer Ther* 14:2896–2900
- Polnaszek N, Kwabi-Addo B, Peterson LE, Ozen M, Greenberg NM, Ortega S, Basilico C, Ittmann M (2003) Fibroblast growth factor 2 promotes tumor progression in an autochthonous mouse model of prostate cancer. *Cancer Res* 63:5754–5760
- Ruggeri B, Singh J, Gingrich D, Angeles T, Albom M, Yang S, Chang H, Robinson C, Hunter K, Dobrzanski P, Jones-Bolin S, Pritchard S, Aimone L, Klein-Szanto A, Herbert JM, Bono F, Schaeffer P, Casellas P, Bourie B, Pili R, Isaacs J, Ator M, Hudkins R, Vaught J, Mallamo J, Dionne C (2003) CEP-7055: a novel, orally active pan inhibitor of vascular endothelial growth factor receptor tyrosine kinases with potent antiangiogenic activity and antitumor efficacy in preclinical models. *Cancer Res* 63:5978–5991
- Sahadevan K, Darby S, Leung HY, Mathers ME, Robson CN, Gnanapragasam VJ (2007) Selective over-expression of fibroblast growth factor receptors 1 and 4 in clinical prostate cancer. *J Pathol* 213:82–90
- Siegel RL, Miller KD, Jemal A (2018) Cancer statistics, 2018. *CA Cancer J Clin* 68:7–30
- Steinemann G, Jacobsen C, Gerwing M, Hauschild J, von Amsberg G, Hopfner M, Nitzsche B, Honecker F (2016) Activity of nintedanib in germ cell tumors. *Anti-Cancer Drugs* 27:89–98
- Weibel ER (1963) Principles and methods for the morphometric study of the lung and other organs. *Lab Invest* 12:131–155
- Xu D, Wang X, Lou Y (2017) Association of endothelin-1 gene single-nucleotide polymorphisms and haplotypes with risk of hormone refractory prostate cancer. *Pharmazie* 72:103–106
- Yamaguchi K, Izaki H, Takahashi M, Fukumori T, Nishitani M, Sutou Y, Uema K, Kawano A, Hamao T, Kanayama HO (2014) Changes in levels of prostate-specific antigen and testosterone following discontinuation of long-term hormone therapy for non-metastatic prostate cancer. *J Med Investig* 61:35–40
- Zar J (1999) *Biostatistical analysis*. Prentice Hall, New Jersey

Publisher's note Springer Nature remains neutral with regard to jurisdictional claims in published maps and institutional affiliations.